

Identification of Barriers to the Movement of the Train

¹Yuri Bekhtin, ¹Petr Krug, ¹Alexey Lupachev, ²Andrey Ostroukh,

¹Sergey Pavelyev and ¹Igor Zhelbakov

¹National Research University "Moscow Power Engineering Institute", Moscow, Russia

²Department of Automation Control Syst., State Technical University, MADI, Moscow, Russia

Abstract: The problems of wavelet-based data and image fusion design for on-board control equipment of the locomotive are highlighted. The fusion scheme using matching pursuit of coherent structures and the fusion scheme using spatial oriented trees are described. The results of modeling and comparison are presented.

Key words: Train, identification of barriers, video cameras, locators, infrared scanning devices, wavelet-transform, image fusion

INTRODUCTION

The last decades are characterized by increasing railroad traffic worldwide. Many countries with developed railroad infrastructures are compelled to implement different systems of functional requirements for monitoring and controlling train movements to provide increased safety. For example, the American Railway Engineering and Maintenance-of-Way Association (AREMA) describes Positive Train Control (PTC) as having these primary characteristics:

- Train separation or collision avoidance
- Line speed enforcement
- Temporary speed restrictions
- Rail worker wayside safety

The same situation is in Russian Federation where the government pays a lot of efforts and does constantly modify the state standards of railroad safety. One of modifications lays in the conception also known as movement authorities. According to http://en.wikipedia.org/wiki/Positive_train_control-cite_note-1 that the train receives information about its location and where it is allowed to safely travel. The equipment on board the locomotive must continually calculate the trains' current speed relative to a speed target some distance away governed by a braking curve. If the train risks not being able to slow to the speed target given the braking curve, the brakes are automatically applied and the train is immediately slowed. The speed targets are updated by information regarding fixed and dynamic speed limits determined by the track profile and signaling system.

Most current implementations also use the speed control unit to store a database of track profiles attached to some sort of navigation system. The unit keeps track of the train's position along the rail line and automatically enforces any speed restrictions as well as the maximum authorized speed. Temporary speed restrictions can be updated before the train departs its terminal or via wireless data links. The track data can also be used to calculate braking curves based on the grade profile. The navigation system can use fixed track beacons or differential GPS stations combined with wheel rotation to accurately determine the train's location on the line accurately within a few feet.

Unfortunately, these technical and organization efforts are not sufficient today. A train traveling at high speed has a tremendous amount of inertia which must be overcome in order to quickly stop it. A quick stop for a train may take up to a half kilometer. Moreover, many barriers and crossings are situated such that a train's driver has little, if any, reaction time to stop a train if he/she is able to recognize barriers as a vehicle, person or animal on rails. Or due to darkness, rain or fog, the train may actually be at the crossing before an object is recognized in the crossing. In this case, it is too late to avoid an accident. And even if a train can be significantly slowed before reaching the barriers, it still may have enough momentum to damage or destroy anything in its path. In addition to the damage or harm possibly inflicted on those outside the train, occupants of the train may also be injured. Crossing accidents often cause some of the cars of the train to derail with people in those cars being injured. People in other railroad cars are often shaken or jolted by the sudden deceleration which takes place during emergency braking resulting in injuries.

Thus, the safety of people due to damage resulting from a collision or sudden stoppage of the train “pushes” to invent new methods of the locomotive speed control. The one way out is to expand railroad safety systems with video detection hardware for viewing railroad barriers and crossings to determine if the barrier does exist or the crossing is clear or whether vehicles, persons, animals or other objects are on the rails. Further, the apparatus creates an alarm signal to a train’s driver notifying him/her if there is any barrier or, one or more of these objects are identified as being in the crossing. This is done so the train can be halted prior to its reaching the crossing, thereby preventing injury to a person or animal or damage to the vehicle, train, or other object in the crossing. We can conclude the next requirements to the provision of such hardware:

- Viewing a railway path and crossing to determine if an object (vehicle, person, animal, other object) is present in a railroad
- Determining if the object is sufficiently sized to cause damage to a railway train approaching the barrier or the crossing
- Halting the train so as not to harm the object, nor to harm the approaching train and its occupants
- Automatically, continuously obtaining an electro-optical image of the railroad path to process and evaluate the image once the approaching train is within the predetermined distance of the barrier or the crossing, the evaluation including a determination as to whether a perceived object exceeds a predetermined minimum size
- Providing an alarm signal to the train’s driver if the evaluation reveals an object as the barrier to validate a received alarm signal and to halt the train only when the alarm signal is validated and to effect halting of the train in response to a validated signal
- Functioning at 24/7 and under all weather conditions
- Providing the algorithmic supply which can be built-in the existing locomotive cabin hardware and does not interfere with the train approach warnings or barriers already in place at the crossing

In accordance with the generally stated situation, the proposed hardware is provided for monitoring a railroad path and crossings for the presence of an object on the rails. To determine if the objects (people, animals, vehicles, other objects) are of a sufficient size to cause damage to the train a television (video) camera and other electro-optical devices (sensors) working in infrared and

ultrasound bandwidths have to be installed onto the locomotive cabin. An image processor processes the images obtained to form a fused image of high quality and then analyzes the barrier appearance. An alarm unit is responsive to an output from the processor to provide an alarm signal to the train’s driver as to the presence of the object on the rails. An alarm on the train is sounded in response to the alarm signal obtained from the on-board equipment. In response to the alarm signal, the train may be halted so that it stops short of the barrier or the crossing. This would prevent injury to people in the crossing, people on the train, the train itself or vehicles or other objects in the crossing.

Therefore, to provide effective functioning at 24/7 and under all weather conditions, development of a new algorithmic supply for the locomotive on-board hardware to process images obtained in different spectrum subbands to create a fused image of high quality is required. It allows the algorithms for object detection and recognition to be efficiently applied to the fused image. This study of the study describes some of our methods to the fusion of multispectral images which are degraded not only by bad weather conditions but also the internal noise of the sensors.

THE WAVELET-BASED FUSION

The fast development of embedded computing systems we are observing nowadays is based on impressive effectiveness of chips, DSP, hardware and software design, etc. However, there are some limitations on simplicity of algorithms, memory size and other computing resources which are still remaining. It is the most related to digital image processing and this work can be considered as an attempt to create a fast and very effective algorithm for fusion of noisy multispectral images.

Image fusion can be referred as the process by which several low resolution images or some of their features obtained by different sensors are combined together to form a single high resolution image. This work focused on development of pixel level fusion algorithms. The well-known algorithms vary from very simple, e.g., image averaging, to very complex, e.g., principal component analysis, pyramid based image fusion and Wavelet Transform (WT) fusion (Stathaki, 2008). The latter has become one of the most popular fusion methods in video camera viewing, remote sensing, medical imagery in recent years and has been standard module in commercial image processing software such as ENVI, PCI,

ERDAS. In all wavelet-based image fusion schemes, the wavelet transforms of the two or more registered input images are computed and then these transforms are combined using any fusion rule.

The pixel level fusion schemes can employ different types of WT (Stathaki, 2008; Li *et al.*, 1995), e.g., the Fast WT (FWT), the Dual-Tree Complex WT (DT-CWT) to obtain a wavelet decomposition of the input images. The wavelet coefficients are then combined using a maximum-selection fusion rule often to produce a single set of coefficients corresponding to the fused image. The maximum-selection scheme selects the largest absolute wavelet coefficient at each location from the input images as the coefficient at that location in the fused image.

As wavelets tend to pick out the salient features of an image, this and more complex schemes such as Rockinger *et al.* (1998) and Burt and Koleszynski (1993) work well with uncorrupted images. Nevertheless, many modern sensors can additionally contribute with specific noises, e.g., fixed pattern noise in infrared devices, speckle in SAR, etc. In the case of noisy images, some filtering procedures should be included in the fusion rules. There are some works related to the fusion of noisy images (Mallat and Zhang, 1993; Ostroukh *et al.*, 2014a, b, 2011). Evidently, the wavelet-based fusion could perform better than convenient methods in terms of minimizing color distortion and de-noising effects. The main problem is to determine appropriate values for certain parameters (such as thresholds) that related to the user.

This work is aimed to submit the fully automatic fusion scheme where the maximum-selection fusion rule is replacing into two ways. The first way is a matching pursuit of so-called coherent structures of noisy images when the maximal correlation between non-linear approximation of any noisy image and the given wavelet basis is achieved (Ostroukh *et al.*, 2014a). The second way is a logical processing of wavelet coefficients belonging to different Spatial Oriented Trees (SOTs) (Shapiro, 1993; Said and Pearlman, 1996). These methods have already been presented in study (Bekhtin and Bryantsev, 2011; Bekhtin *et al.*, 2013) further a short description of the suggested methods with respect to the problem of barrier detection is provided.

THE FUSION SCHEME USING MATCHING PURSUIT OF COHERENT STRUCTURES

The method of extracting coherent structures (Berger *et al.*, 1994) using the library of local trigonometric bases and wavelet packets has been successfully applied

to recovering the corrupted musical records. For the sake of simplicity, this scheme was modified for fusion of 2D signals where noisy images form the library and an estimator of the correlation coefficient is computed with only the one wavelet basis chosen by the user before. To avoid artifacts in the fused image a procedure known as the Shift Invariant Discrete Wavelet Transform (SI-DWT) (Otazu *et al.*, 2005) is applied.

Let $Y = X + Z$ be a noised original image X containing I pixels which is undergone to be decomposed in several levels by WT with the given wavelet basis. Noise Z in Y , with variance σ_z^2 can be determined as components of the decomposed image w_{ξ_k} , $k = 1, \dots, I$, not having a strong correlation with the given basis. If I is relatively large then for any orthonormal wavelet basis there is existing the probability up to 1 that (Mallat and Zhang, 1993):

$$\frac{\max_{1 \leq k \leq I} |w_{\xi_k}|}{\|Z\|} \leq \frac{\sqrt{2 \ln I} \sigma_z}{\sqrt{I} \sigma_z} = \frac{\sqrt{2 \ln I}}{\sqrt{I}} = \rho_1 \quad (1)$$

Here is assumed that Z is normal (Gaussian) process (white noise) with zero mean. The parameter ρ_1 can be considered as the high bounded estimator of the correlation coefficient for correlation between Gaussian noise and any given wavelet basis and as it is seen from Eq. 1 this estimator does not depend on noise variance. It has been experimentally proven by the first researcher that the theoretical value of ρ_1 is also the highest asymptote of the correlation coefficients for correlation between Daubeshies wavelets, symmlets, few biorthogonal wavelets and noises having different probability density functions (pdf) and their combinations such as log-normal, exponential, Gamma-distributed, etc.

On the other hand, the correlation coefficient for correlation between an input image and the given wavelet basis can be computed using wavelet coefficients w_{Y_i} , $1 \leq i \leq I$ of the observed image Y :

$$\rho(Y) = \frac{\sup_{1 \leq i \leq I} |w_{Y_i}|}{\|Y\|} \quad (2)$$

The correlation coefficient Eq. 2 is computed on the data of the noised image and it can help to choose the best basis from the library of bases only. In order to extract useful components from the noised image it is necessary to have more flexible scheme. It is known from the theory of wavelets (DeVore, 1998) that the non-linear approximation of any signal being decomposed by

wavelet transform is referred as inverse wavelet transform W^{-1} for first (significant) M wavelet coefficients after their sorting:

$$\hat{X} = \sum_{k=1}^M W^{-1} \{w_{Y_k}\} \quad (3)$$

Where:

$$|w_{Y_k}| \geq |w_{Y_{k+1}}|, \forall k \in [1, \dots, I] \quad (4)$$

Hence, a coherent structure of the input image is determined according to the rule (Mallat and Zhang, 1993):

$$\rho(Y_k) = \frac{|w_{Y_k}|}{\|Y\|} > \rho_1, 1 \leq k \leq M \quad (5)$$

Having any value of M the rest image Y_M can be calculated as the difference between the input image and the pseudo image obtained by means of the inverse wavelet transform for the coherent structures:

$$Y_M = Y - \sum_{k=1}^M W^{-1} \{w_{Y_k}\} = \sum_{k=M+1}^I W^{-1} \{w_{Y_k}\} \quad (6)$$

The rest image Y_M can not be recognized as a noise if the next inequality is true:

$$\rho^2(Y_M) = \frac{|w_{Y_M}|^2}{\sum_{k=M+1}^I |w_{Y_k}|^2} > \rho_{1-M}^2 \quad (7)$$

The estimator \hat{X} of the original image is the sum of M coherent structures Eq. 3. It is worth to mark that pursuit of the coherent structures looks like hard thresholding of the wavelet coefficients with the threshold (Mallat and Zhang, 1993):

$$\tau = \rho_{1-M} \sqrt{\sum_{k=M+1}^I |w_{Y_k}|^2} \quad (8)$$

It is assumed that there are L noisy images of the same scene registered by sensors operating in different spectral bandwidths. They form the library of the input images $\Lambda = \{Y^1, Y^2, \dots, Y^L\}$. In order not to have a routine procedure each image should be decomposed with the one wavelet-basis chosen by the end-user from the library of wavelet bases. Choice of the suitable wavelet basis can be done by different methods based on cost functions,

e.g., using the estimator (Eq. 2) $\rho(Y_\tau)$, $\tau = 1, \dots, L$ of the coefficient correlation between the input image Y^τ , $\tau = 1, \dots, L$ and any wavelet basis from the library of bases. Because the input images contain one and the same scene there are cases when one and the same wavelet basis can be chosen for few images. It usually happens if the quantity of images in the library Λ is relatively small, e.g., $L = 2, L = 3$ and/or images are registered from the sensors working in tight bandwidths without wide guard gaps. In spite, our experience has shown that extracting of the coherent structures is stabile in such cases.

The input images have low resolutions because of sensors' noises. When the properties of the noises are unknown the pursuit of the coherent structures can be considered as thresholding of wavelet coefficients with the threshold (Eq. 8) the value of that is changing adaptively. The main idea of the proposed fusion scheme is to keep up those of coherent structures of images which are the best under some criterion and the result fused image is the sum of the saved coherent structures (Eq. 3).

To pursuit the best coherent structure of the input images such coherent structure is chosen corresponding to the image with number α in the library which is minimizing the cost function:

$$C(Y^\alpha) = \min_{\tau} C(Y^\tau), \tau = 1, \dots, L \quad (9)$$

Where:

$$C(Y^\tau) = \sum_{i=1}^I \Phi \left(\frac{|w_{Y_i^\tau}|^2}{\|Y^\tau\|^2} \right) \quad (10)$$

As it is seen from Eq. 9 the choice of the best coherent structure depends on the kind of the function Φ . We choose the entropy function:

$$\Phi(u) = -u \ln u, u \geq 0 \quad (11)$$

During analysis of noisy images it is impossible to exactly indicate which image along with its components is dominating in typical fusion schemes. The proposed fusion scheme can be iteratively applied to all of images from the library if we put $Y_M = Y$ for the next step. It allows to consequently correct the fused image because the best coherent structure can be extracted from any rest image among the rest images on the current iteration. The proposed fusion algorithm contains the next steps:

1. To form the library of multispectral images where all or some of them are corrupted by specific noises of sensors
2. To choose the best wavelet basis for each image under some criterion by the end-user
3. To put $Y_M^\tau = Y^\tau$, $\tau = 1, \dots, L$
4. To perform SI-DWT for each image from the library with the given wavelet bases and to save arrays of wavelet coefficients
5. To sort the wavelet coefficients in accordance with Eq. 4
6. To pursuit coherent structures of the images using Eq. 7 and to find the value of M
7. To restore the nonlinear approximations \hat{x} and the rest images Y_M^τ by the inverse wavelet transform
8. To compute the values of the cost function Eq. 10 to choose using Eq. 9 and keep up the best coherent structure \hat{x}^* in memory
9. To correct the saved image calculated on the previous iteration with the new nonlinear approximation \hat{x}^*
10. If $M = 0$ then to stop, the fused image has been already cumulated in memory and can be displayed; otherwise go to the step 3

THE FUSION SCHEME USING SPATIAL ORIENTED TREES

Usually, SOTs are used in wavelet compression techniques such as EZW, SPIHT (Shapiro, 1993; Said and Pearlman, 1996). The calculation of SOTs is very fast in the case of using the special compiled software. The one method of applying SOTs to despeckling of SAR image described by Peng and Chan (2001) is assumed to threshold the wavelet coefficients where the threshold value is calculated on the base of an estimator of the noise variance in SOTs. Nevertheless, a thresholding contributes so-called ringing artifacts in the fused image that decreases some quality parameters such as Peak-to-Signal-Noise Ratio (PSNR) and the Structural Similarity Index Measure (SSIM). Therefore, to avoid the artifacts in the fused image a logical procedure of processing is applied to keep the useful content of the input images.

In order to reduce the computational cost of the algorithm, the fast wavelet transform FWT or the Mallat's scheme of the wavelet decomposition (Mallat and Zhang, 1993) is chosen. In the two-dimensional case, the FWT is the decomposition of the input image on the branches of approximation (low-frequency sub-band) and the details (high-frequency sub-bands) which are calculated on horizontal, vertical and diagonal directions at each level of the decomposition.

It is known that the wavelet compression of images with algorithms such as EZW, SPIHT (Shapiro, 1993; Said and Pearlman, 1996) is based on representation of the original image in the form of a set of Spatial-Oriented Trees (SOTs). In this representation, all of wavelet coefficients are ordered in the form of SOTs, the roots of which are the points of approximation, i.e., the low-frequency sub-band. The root of the point corresponding to the scaling function has three children.

All other parent-points corresponding to the chosen wavelet have four offspring. The points of the last level (leaves) do not have descendants. According to the algorithms of EZW, SPIHT, the nodes of the tree are consequently reviewed from the parent to the offspring and then it is made a decision about thresholding the descendants of this node. If the value of the wavelet coefficient turns out to be below the threshold (so-called "the dead zone") then this coefficient is considered to be insignificant ("cut off the branch") and the one is replaced by zero (hard thresholding of wavelet-coefficients). The sequence of nodes analysis is being built as the recursive zigzag from the parent to the offspring. In compression techniques, the significant wavelet-coefficients are then undergone by scalar uniform quantization and finally are statistically encoded.

Let there be L noisy images of the same scene which received by video sensors in different spectral bandwidths and which form a library of input images $\Lambda = \{Y^1, Y^2, \dots, Y^L\}$. To reduce the computational cost each image is decomposed with a single wavelet basis selected by an end-user from the available library of wavelet bases. The choice of the appropriate wavelet basis can be made through various cost functions, for example, using the estimator of the coefficient of correlation between the input image Y^τ , $\tau = 1, \dots, L$ and any wavelet basis of the library. For the sake of simplicity, one and the same wavelet basis has been chosen for all of the images because the input images contain one and the same scene.

Each of the fusing images has its own set of SOTs which differ by a dynamic rate of the wavelet coefficients depending on the variance and the probability density function (pdf) of the noise. Figure 1 shows the behavior of the normalized wavelet coefficients ($i = 1, \dots, 64$) obtained by the three-level FWT (i.e., $Q = 3$) for one of 4096 SOTs with number 10 for the test image sized 512×512 in the absence of noise (curve 1) and when noise is affected for additive Gaussian noise (curve 2), multiplicative noise with exponential pdf (speckle noise) (curve 3) and impulse noise (curve 4). Normalization leads to the elimination of signal-noise dependency that allows us to analyze the SOT wavelet coefficients regardless of the level and subband of FWT.

One can see from Fig. 1 that the differences between the decay curves of the SOT wavelet coefficients of the noisy pictures and the "ideal curve" corresponding to the undistorted image have a chaotic character which is especially apparent in the area of the "high-frequency" wavelet coefficients responsible for the details of the image. It should be noted that the traditional maximum

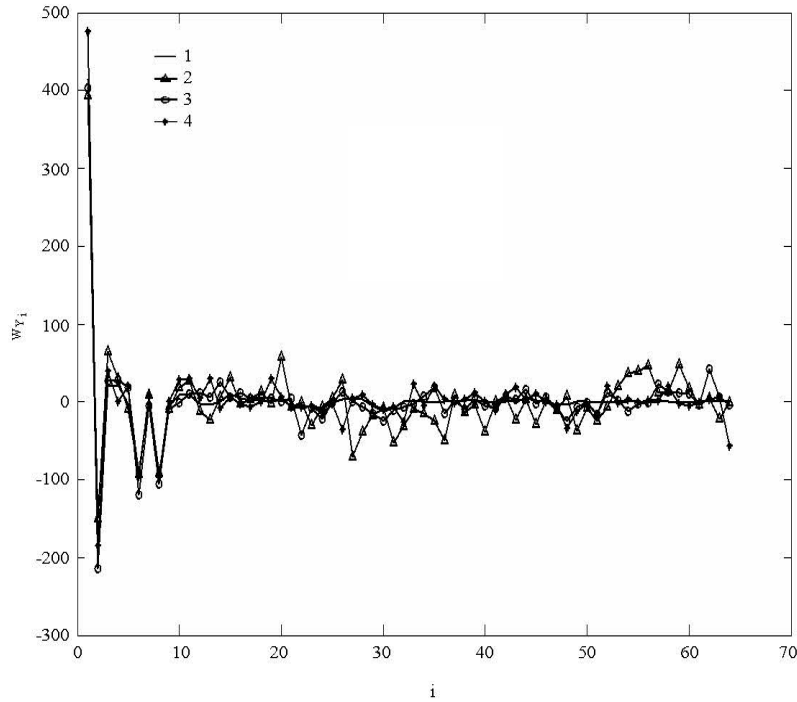


Fig. 1: The normalized wavelet coefficients ($i = 1, \dots, 64$) obtained by the three-level FWT for one of 4096 SOTs with number 10: free of noise (curve 1), additive Gaussian noise (curve 2), multiplicative noise with exponential pdf (speckle noise) (curve 3) and impulse noise (curve 4)

selection fusion rule here is not working properly; on the contrary in order to preserve the details in the fused image, it is desirable to keep the wavelet coefficients with destroys the useful content that is stored in the coefficients. Moreover, high threshold values lead to the appearance of ringing artifacts in the fused image.

The approximation wavelet coefficients have large values due to the property to accumulate the signal energy of the FWT; hence, the signal-to-noise ratio is relatively large for the approximation. Then, it is needed to separately process the approximation and details. Moreover, the results of the modeling have shown that the wavelets coefficients of details can be also divided into two parts: so-called the middle frequency set and the high frequency set of the coefficients. Therefore, three sets of wavelet coefficients in each SOT should be separately processed by three different algorithms. It makes a principal difference to the previous works.

The mean for the approximation wavelet coefficients is calculated and a fast one-dimensional Lee filter is applied to the middle frequency wavelet coefficients.

Thus, the proposed fusion method of noisy images has an empirical character and comprises an attempt to find out a compromise between controversial requirements:

1. Calculate the FWT of noisy multispectral images with the given number of levels (at least three) using one of the wavelet bases
2. Convert arrays of the wavelet coefficients in the form of sets of SOT vectors:

$$SOT^{\tau}(j, k), \tau = 1 \dots L, 1 \leq j \leq N, 1 \leq k \leq K$$

where, N is the number of a SOT, K is the number of wavelet coefficients; for example, if an image has size of 512×512 then for $Q = 3$ we obtain $N = 4096$, $K = 64$

3. Generate vector contained the first wavelet coefficients for all SOTs:

$$P = \max_{\tau} \{SOT^{\tau}(j, 1)\}, 1 \leq j \leq N, \tau = 1, \dots, L$$

4. Normalize the wavelet coefficients of SOTs
5. Process the sets of approximation and middle wavelet coefficients of each SOT. For example, in the case of a three-level wavelet transform there will be the first of four coefficients of SOT
6. Search for the minimal wavelet coefficients among the remaining coefficients belonging to different SOTs by logical operation of comparison
7. Generate a new SOT using the found wavelet coefficients as the results of steps 5 and 6
8. Execute de-normalization, i.e. to multiply with the vector P which is found on step 3
9. Perform the inverse conversion on the received SOTs into the arrays of wavelet coefficients
10. Perform the inverse wavelet transform on the arrays of wavelet-coefficients and generate the fused image

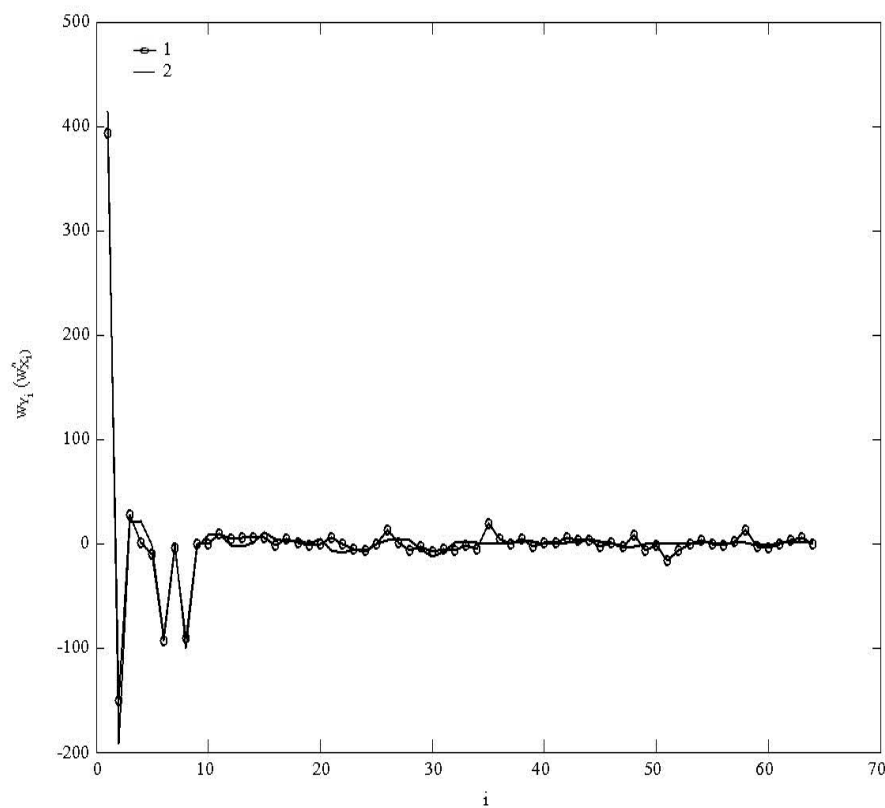


Fig. 2: The synthesized (1) and “ideal” (2) curves for the SOT wavelet coefficients

The example of the modeled execution of the suggested algorithm for the SOT with number 10 is shown on Fig. 2. The figure shows that the curves are very close to each other; hence, we can expect a significant noise reduction and lack of ringing artifacts in the fused image.

MODELING AND COMPARISON RESULTS

At this moment large amount of computer modeling data proves the effectiveness of the suggested fusion schemes. Images registered by video cameras, locators with microwave illumination, infrared scanning devices have been used. Some pictures were obtained in different neighboring bandwidths. Visual observations showed that there is significant improvement of the fused image quality in comparing with the pre-filtering and well-known fusion schemes.

Figure 3 contains the results of simulation modeling for the typical railroad scene. A person crossing the rails is practically invisible for a locomotive driver under additive Gaussian distortions (Fig. 3b). Also, it is difficult to make a decision in the case of impulse noise shown on Fig. 3c. The situation is much worse for the algorithms

Table 1: Results of comparison

Images	PSNR (dB)	SSIM
Corrupted by additive Gaussian noise with $\sigma_s^2 = 34$	18.1	0.7045
Corrupted by multiplicative noise with exponential pdf, $\sigma_s^2 = 56$	16.4	0.4215
Fused by averaging	17.8	0.5633
Fused by maximum-selection fusion rule	18.5	0.5547
Fused by maximum-selection fusion rule with preliminary hard thresholding	19.4	0.7322
Fused by the selected suggested fusion rule	26.5	0.8945

which make decisions regarding train speed decreasing and/or stoppage automatically. The fused image allows both the locomotive driver and embedded alarm software to make the right decision.

Figure 4-6 demonstrate the effectiveness of the suggested fusion algorithms when the normalized cross-correlation between video and infrared images is about 0.5, i.e., there are two different images of the one and the same scene. It happens when cameras or sensors operating in different spectral subbands have different spatial resolutions. One can see from Fig. 4-6 and Table 1 that the proposed method provides better image enhancement both visually and numerically under the PSNR and SSIM criteria.

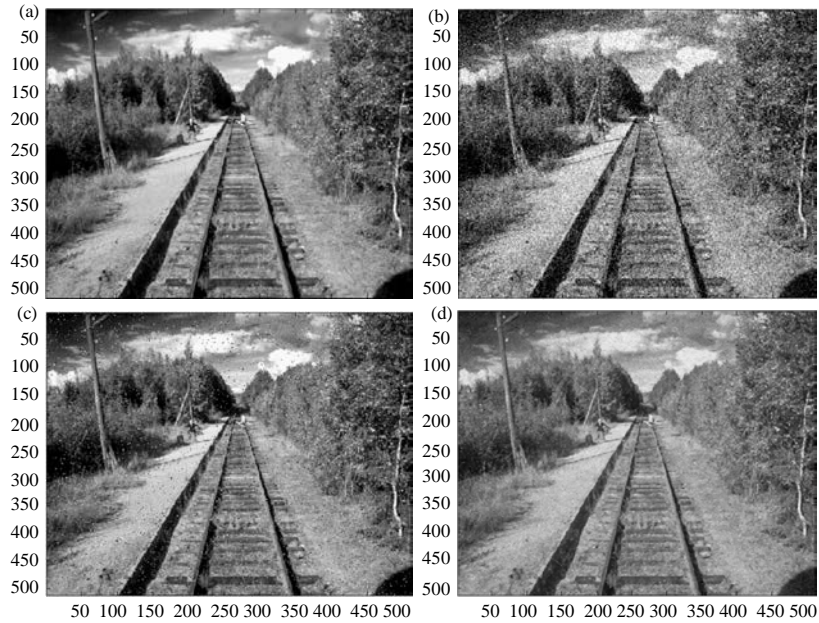


Fig. 3: The results of modeling: a) the undistorted image; b) the image distorted by additive Gaussian noise; c) the image distorted by impulse noise and d) the fused image

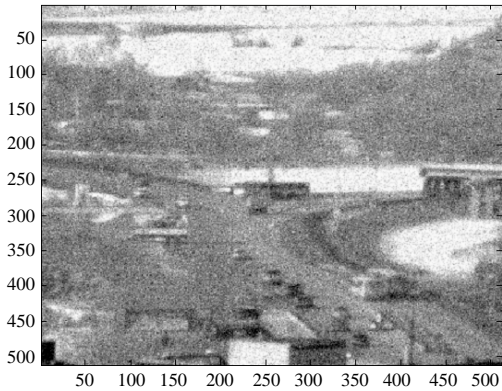


Fig. 4: The noised video image

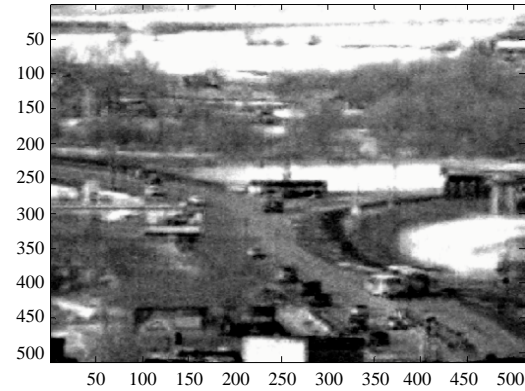


Fig. 6: The fused image

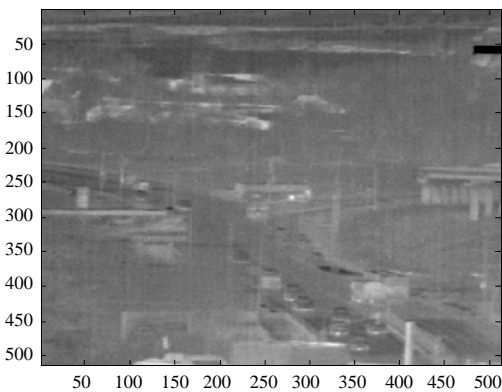


Fig. 5: The infrared image

CONCLUSION

Aggregation of the proposed fusion methods within the locomotive hardware is suggested to increase the effectiveness of the following processing algorithms for object detection and recognition.

The choice of the fusion algorithm depends on the current conditions of viewing. Experimental results have shown that the first fusion scheme works perfectly well under daylight and when the distance between the head of the train and the barrier is relatively large, for example, when the train moves on direct part (without turns) of the railroad path. Otherwise, the second fusion algorithm works better under bad weather conditions. At the current

moment, the suitable method is being explored to automatically differ situations when and which of the proposed fusion algorithms to apply.

ACKNOWLEDGEMENTS

The research was carried out with financial support of the Ministry of Education and Science of the Russian Federation in the framework of the Agreement No. 14.574.21.0047, 19.06.2014.

REFERENCES

- Bekhtin, Y.S. and A.A. Bryantsev, 2011. Matching pursuit of coherent structures during wavelet-based fusion of noisy multispectral images. Proceedings of 11th International Conference on Pattern Recognition and Information Processing, May 18-20, 2011, Minsk, Belarus.
- Bekhtin, Y.S., A.A. Bryantsev and D.P. Malebo, 2013. Wavelet-based fusion of noisy multispectral images using Spatial Oriented Trees. Proceedings of the 2nd Mediterranean Conference on Embedded Computing (MECO), June 15-20, 2013, Budva, Montenegro, pp: 113-116.
- Berger, J., R.R. Coifman and M.J. Goldberg, 1994. Removing noise from music using local trigonometric bases and wavelet packets. *J. Audio Eng. Soc.*, 42: 808-818.
- Burt, P.J. and R.J. Koleszynski, 1993. Enhanced image capture through fusion. Proceedings of 4th International Conference on Computer Vision, May 11-14, 1993, Berlin, Germany, pp: 173-182.
- DeVore, R.A., 1998. Non-linear approximation. *Acta Numer.*, 7: 51-150.
- Li, H., B.S. Manjunath and S.K. Mitra, 1995. Multisensor image fusion using the wavelet transform. *Graphic. Models Image Process.*, 57: 235-245.
- Mallat, S.G. and Z. Zhang, 1993. Matching pursuits with time-frequency dictionaries. *IEEE Trans. Signal Process.*, 41: 3397-3415.
- Ostroukh, A., S. Vasuhova, M. Krasnyanskiy and A. Samarutunga, 2011. Study the prospects and problems of integration of human-computer: Artificial intelligence, robotics, technological singularity and virtual reality. *Prospects Sci.*, 4: 109-112.
- Ostroukh, A., V. Nikonov, I. Ivanova, T. Morozova, K. Sumkin and D. Akimov, 2014a. Development of contactless integrated interface of complex production lines. *J. Artifi. Intell.*, 7: 1-12.
- Ostroukh, A., V. Nikonov, I. Ivanova, T. Morozova and V. Strakhov, 2014b. Distributed system of real time head gesture recognition in development of contactless interfaces. *Middle East J. Scient. Res.*, 20: 2177-2183.
- Peng, C. and A. Chan, 2001. Speckle noise removal in SAR image based on SOT structure in wavelet domain. Proceedings of the IEEE Transactions on Geoscience and Remote Sensing Symposium, July 9-13, 2001, Sydney, NSW, pp: 3039-3041.
- Rockinger, O., T. Fechner and D.B. Ag, 1998. Pixel-level image fusion: The case of image sequences. *SPIE Proc.*, 3374: 378-388.
- Said, A. and W.A. Pearlman, 1996. A new fast and efficient image codec based on set partitioning in hierarchical trees. *IEEE Trans. Circ. Syst. Video Technol.*, 6: 243-250.
- Shapiro, J.M., 1993. Embedded image coding using zerotrees of wavelet coefficients. *IEEE Trans. Signal Process.*, 41: 3445-3462.
- Stathaki, T., 2008. Image Fusion: Algorithms and Applications. Academic Press, New York, Pages: 519.